

**Distribution in flowing reaction-diffusion systems**Atsushi Kamimura,<sup>1,2</sup> Hans J. Herrmann,<sup>1,3</sup> and Nobuyasu Ito<sup>2</sup><sup>1</sup>*Computational Physics for Engineering Materials, IfB, ETH Zürich, Schafmattstrasse 6, CH-8093 Zürich, Switzerland*<sup>2</sup>*Department of Applied Physics, Graduate School of Engineering, The University of Tokyo, 7-3-1, Hongo, Bunkyo-ku, 113-8656 Tokyo, Japan*<sup>3</sup>*Departamento de Física, Universidade Federal do Ceará, 60451-970 Fortaleza, CE, Brazil*

(Received 24 September 2008; revised manuscript received 26 April 2009; published 28 December 2009)

A power-law distribution is found in the density profile of reacting systems  $A+B \rightarrow C+D$  and  $2A \rightarrow 2C$  under a flow in two and three dimensions. Different densities of reactants  $A$  and  $B$  are fixed at both ends. For the reaction  $A+B$ , the concentration of reactants asymptotically decay in space as  $x^{-1/2}$  and  $x^{-3/4}$  in two dimensions and three dimensions, respectively. For  $2A$ , it decays as  $\log(x)/x$  in two dimensions. The decay of  $A+B$  is explained considering the effect of segregation of reactants in the isotropic case. The decay for  $2A$  is explained by the marginal behavior of two-dimensional diffusion. A logarithmic divergence of the diffusion constant with system size is found in two dimensions.

DOI: [10.1103/PhysRevE.80.061132](https://doi.org/10.1103/PhysRevE.80.061132)

PACS number(s): 05.40.-a, 05.60.-k, 82.20.-w

**I. INTRODUCTION**

In engineering and industrial applications in chemical plants, controlling reactions is essential for efficient production of chemicals. The field of microreaction technology has been taking advantages associated with reaction miniaturization [1]. A microreactor where reactions take place in a microscale to milliscale confinement is a common device and it is usually a continuous flow reactor where chemical reactions run in a flowing stream rather than in a batch production. The reactor is typically tube like and reactants are continually added to the input of the reactants and products continually collected from the output. Subsequent processing of intermediates and chain reactions is also favored in this manner. As the reactants are continually flowing in one direction, the reaction rate depends on the residence time in the reactor which varies with the flow rate and the volume and length of the reactor. Although the adjustment of physical and geometrical parameters is essential to obtain a necessary amount of products in the output, understanding the reaction dynamics and the control in the microscopic flowing stream are still at a phenomenological level.

On the other hand, theoretical studies show that reactive and transport processes in a low-dimensional space can yield striking effects. Microscopic fluctuations can strongly influence the collective behavior and lead to a breakdown of conventional reaction-diffusion equation. Since the pioneering work of Ovchinnikov and Zeldovich [2], two species annihilation processes  $A+B \rightarrow 0$  have been attracting much interest and been widely investigated. The main point is that, if initially the reactants are randomly distributed in equal proportions, density fluctuations between  $A$  and  $B$  cause segregation and formation of clusters of single species. The reactions occur along the boundaries of the clusters and consequently they proceed slower than in homogeneous systems. Actually, the densities of  $A$  and  $B$  asymptotically approach  $\rho_A(t) = \rho_B(t) \sim t^{-d/4}$  if the spatial dimensionality  $d$  is less than 4 [3]. These effects have been also examined in isolated systems using numerical simulations on regular lattices [3], fractals [4], restricted geometries [5], and complex networks [6].

The purpose of this paper is to examine the effect of fluctuations in the flowing condition of reactors by performing a nonequilibrium molecular-dynamics (MD) simulation. From the application point of view, on a macroscale such effects might be diminished by introducing mixing stirrer in the reactors. However, on the microscale, mixing is dominated by molecular diffusions, which is particularly relevant for reaction miniaturization. For this purpose, we consider a continuous flow between reservoirs of high-density reactants and low-density products and examine how reactants distribute in between. The reservoirs are attached only to the boundaries of our system and microscopic dynamics in the bulk follows usual Newtonian dynamics; no *a priori* asymmetries are included. In the present paper, we focus on one-directional flow, and we will not consider the effects of tubular geometries. As we will explain later, we impose periodic boundary conditions in the perpendicular directions to the flow instead of fixed walls.

The first point we note here is that the system is a non-equilibrium open system. A first approach to examine reaction-diffusion systems is to write down mean-field rate equations. However, the rate equations assume that the system is near equilibrium. As we will explain later, the dynamics of our model is Newtonian and does not assume phenomenological rate equations. We note that in the simplest mutually catalyzing systems, rate constants can show non-Arrhenius algebraic dependence on reaction energy in non-equilibrium conditions [7,8].

The second point is low dimensionality. While dimensionality is relevant to the segregation of  $A+B$  reactions, in systems with  $d \leq 2$ , diffusion processes are anomalous. In the isotropic case of single species annihilation  $2A \rightarrow \text{inert}$  in two dimensions, numerical studies show that the density decays as  $\log t/t$  in which a logarithmic factor is added to the mean-field solution  $1/t$  [9]. Further, in driven diffusive systems, density fluctuations spread faster than normal diffusive motions [10], and it is numerically observed in the reaction  $A+B$  that the densities decay as  $t^{-1/3}$ , while in the isotropic diffusive case they decay as  $t^{-1/4}$  in one dimension [11,12].

While most of the numerical studies have been performed with Monte Carlo simulations of lattice-based dynamics, MD

simulations have been also a powerful and reliable tool for investigating transport processes at the microscopic scales using hard sphere fluids [9]. In particular, nonequilibrium MD methods enable us to directly apply relevant driving forces. For isothermal mass transport, the gradient of chemical potential acts as the driving force. We note that, in recent nonequilibrium studies of heat conduction, anomalous behavior of transport coefficients has been observed in low dimensions using hard sphere fluids [13].

## II. MODEL

We consider hard sphere fluids. The particles have uniform radius ( $\sigma=0.5$ ) and masses ( $m=1$ ). The geometries of our systems are a rectangular plane  $L_x \times L_y$  ( $L_x > L_y$ ) in two dimensions and a parallelepiped box  $L_x \times L_y \times L_z$  ( $L_x > L_y = L_z$ ) in three dimensions, respectively. At both ends of  $x$  direction, we control the densities of particles to be high and low, respectively, which we will explain later. In the  $y$  and  $z$  directions, periodic boundary conditions are imposed. Instead of fixed walls because we first want to see how the reaction occurs in a one-directional flow, not in a quasi-one-dimensional geometry so that we want to reduce the effects of walls. The particles elastically collide with each other if the distances between them become equal to the diameter of the particles. At the collision, the velocities of the colliding particles are changed according to the conservation of kinetic energy and momentum.

The simulations are carried out by event-driven molecular dynamics, in which simulation steps are determined by the collision events. In every step, we search the earliest collision time and the positions and velocities of the involved pair of particles. Between collisions, we move every particle on a straight line with its velocity as the velocities of the particles do not change except during collision events. After the movements, we change velocities of the colliding pair according to the conservation laws. We repeat these procedures in the simulations. In our case, simulating hundreds to thousands of particles, this method is more efficient than time-step-driven methods in which one has a constant time interval.

At both ends in the  $x$  directions, the number of particles is controlled. Before explaining how we control the number of particles  $n$ , let us consider distributions of  $n$  particles in a subsystem of a system which contains a fixed large number of particles  $N$ . We denote by  $p$  the probability that a particle is in the subsystem. The probability that the number of particles in the subsystem is  $n$  is given by the binomial distribution as

$$P_N(n) = \binom{N}{n} p^n (1-p)^{N-n}.$$

In the limit  $p \ll 1$  and  $n \ll N$ , one obtains a Poisson distribution of mean  $pN$ .

We assume that particle reservoirs are attached to both ends in the  $x$  direction of our systems. We consider two slices of width  $\Delta x$  at each end in the  $x$  direction from  $x=0$  to  $\Delta x$  and from  $x=L_x - \Delta x$  to  $L_x$ . Here we fix  $\Delta x=5$ . The volume of the slice  $V_S$  is  $V_S = \Delta x \times L_y$ , and  $\Delta x \times L_y \times L_z$  in two and three

dimensions, respectively. In these slices, we control the number of particles as follows. For the left ( $x=0$ ) and right ( $x=L_x$ ) slices, we fix the average densities of particles to be  $\bar{\rho}_L$  and  $\bar{\rho}_R$ , respectively, with  $\bar{\rho}_L > \bar{\rho}_R$ . Particles in the slices can move into the bulk of the system and vice versa. In each simulation step, we randomly choose a number  $\hat{N}_L(\hat{N}_R)$  from a Poisson distribution of a mean  $\bar{N}_L = \bar{\rho}_L V_S$  ( $\bar{N}_R = \bar{\rho}_R V_S$ ). If the number of particles  $N_L(N_R)$  is greater than  $\hat{N}_L(\hat{N}_R)$ , we randomly remove particles from the slice by  $N_L - \hat{N}_L$  ( $N_R - \hat{N}_R$ ). If  $N_L(N_R)$  is less than  $\hat{N}_L(\hat{N}_R)$ , we add particles at random positions in the slices. Velocities of the added particles are chosen randomly from a Maxwell distribution of temperature  $T=1$ . Every particle colliding with the boundaries  $x=0$  and  $L_x$  elastically bounces back. Here, it may be confusing that we put walls at the ends when we compare our model with previous lattice-based models in which diffusion (hopping) is asymmetric, i.e., reactants prefer to move to a specific direction [11,12]. In such cases, periodic boundaries in the  $x$  direction are used to realize a flow. But in the bulk of our system, we do not include any asymmetry and as explained later, it is the difference between the fixed densities which originates the flow of particles.

Now we explain reaction processes. To implement reaction processes, we assume that each particle belongs to a species  $A$ ,  $B$ ,  $C$ , and  $D$ . We implement the processes  $A+B \rightarrow C+D$  by considering that every collision event of reactants  $A$  and  $B$  is reactive and instantaneous so that their identities change to  $C$  and  $D$ . We assume that  $C$  and  $D$  are inert so that they will not be involved in reactions, however, they will collide with the remaining reactants  $A$  and  $B$ . In previous lattice-based models considering the case  $A+B \rightarrow 0$  [3,5], the motion of  $A$  and  $B$  is hopping (diffusion) between sites so that, neglecting the existence of the inert products, the reactants can continue the diffusive motion as before. However, in our hard sphere system, collisions with other particles realize diffusive motions of reactants. If we neglect the products, reactants would only change their velocities at reactive collisions and the situation would be close to ballistic annihilations. However, by considering  $C$  and  $D$ , the reactants experience nonreactive collisions. Since these products are produced by reactions their densities increase which may cause some effects on the diffusions. However, as we will show later, in the asymptotic region, the densities of products are ten to hundred times greater than that of reactants so that the relative increase is small and the effect is not relevant to the macroscopic behavior. We assume that in the left high-density slice, the added particles are reactants  $A$  and  $B$  with equal probabilities. In the right slice, they have products  $C$  and  $D$  in the same manner. Using these boundary conditions, we consider how reactants distribute between the high-density reactants' and low-density products' reservoirs.

We start our simulations from initial conditions in which particles of  $A$  and  $B$  are randomly distributed in equal proportion. The system attains a steady state when inflow and outflow of particles balance.

## III. RESULTS

In Fig. 1, we show the average density of reactants in the steady state. When particles move in this geometry without

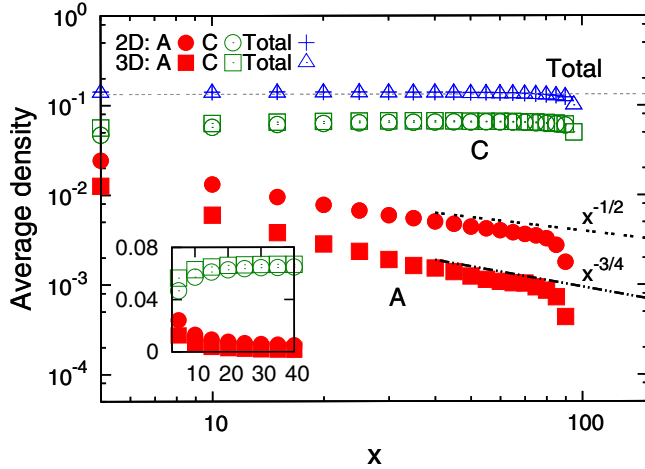


FIG. 1. (Color online) Log-log plot of spatial distributions of reactants of the reaction  $A+B \rightarrow C+D$  in two and three dimensions. The parameters are fixed as  $\bar{\rho}_L=0.155$  and  $\bar{\rho}_R=0.111$ ,  $L_x=100$ , and  $L_y=L_z=10$ . The lines  $x^{-1/2}$  and  $x^{-3/4}$  are also shown. In the inset, we show a zoom of the profile in which we can see the decrease in reactants and an increase in products.

reactions, they show constant profiles (labeled as total in the figure). The profile depends on the density differences  $\bar{\rho}_L - \bar{\rho}_R$  and does not depend on the system size  $L_x$ . The left end  $x=5(\Delta x)$  of the figure corresponds to a boundary between the left high-density slice and the bulk of the system. As we can see, the reactants  $A$  and  $B$  asymptotically decay as  $\rho_A = \rho_B \sim x^{-1/2}$  and  $x^{-3/4}$  in two and three dimensions, respectively. In the inset, we show a zoom from  $x=5$  to  $40$  in which we can see that the decrease in the reactants produces an increase in  $C$ .

Although the velocities of the particles added in the two slices are given by the isotropic Maxwell distribution, particles flow in the  $x$  direction with a constant average velocity due to the pressure difference between the slices. In fact, we confirmed in the bulk that the velocity distribution in the  $x$  direction follows the Maxwell distribution around a nonzero value. If particles are constantly flowing in the  $x$  direction, mean-field solutions of  $\rho_A$  and  $\rho_B$  will approach  $x^{-1}$  because reactants will decay as  $t^{-1}$  while particles move as  $x \sim vt$ , where  $v$  denotes their velocity. However, in reality they decay slower, suggesting the appearance of fluctuations, i.e., the segregation of reactants.

To see clear segregation in this geometry, we study larger systems and show several snapshots of the reactants at different times in Fig. 2. The left end is the high-density side. Black and white circles denote  $A$  and  $B$ , respectively. We can see that the mixed reactants near the left side start to flow separately to the right. We note that although for different setups, segregation effects have been also observed in other systems [5,9]. We also note here that the exponent is calculated from clearer data obtained in smaller system in Fig. 1 since the data are averaged in the steady state it is possible to take more averages in smaller systems with the same computer efforts.

To confirm this segregation of reactants, we calculate the particle-particle correlation function of species  $A-A$  and  $A-B$ . We define the function  $g_{AA}^x(r)$  and  $g_{BA}^x(r)$  as

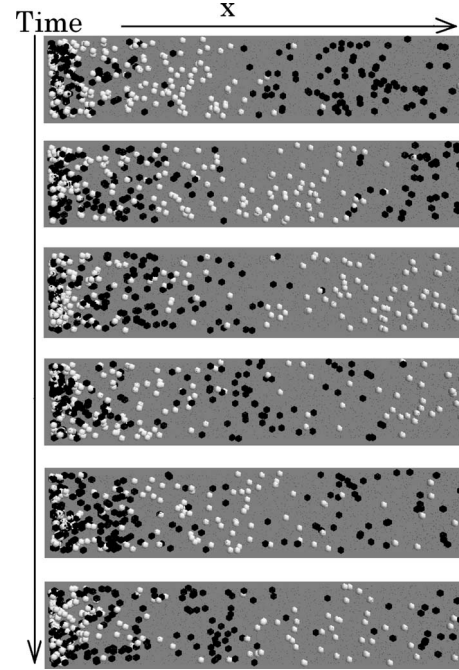


FIG. 2. Snapshots in our geometry. The parameters of the simulation are  $L_x=800$  and  $L_y=100$ . Black and white circles denote  $A$  and  $B$ , respectively. The left end corresponds to the high-density side. Radii of the reactants are shown enlarged to make the presentation clearer.

$$g_{AA}^x(r) = \frac{1}{\bar{\rho}_A} \frac{n_{AA}(r)}{2\pi r}, \quad g_{BA}^x(r) = \frac{1}{\bar{\rho}_B} \frac{n_{BA}(r)}{2\pi r}, \quad (1)$$

where  $\bar{\rho}_A$  and  $\bar{\rho}_B$  denote average densities of  $A$  and  $B$  and  $n_{AA}(r)$  and  $n_{BA}(r)$  denote the number of  $A$  and  $B$  particles at distance  $r$  from a reference particle  $A$ , respectively. In Fig. 3, we show  $g_{AA}^x(r)$  for  $x=5, 6, \dots, 13$  arranged in the direction of the arrow. The  $g_{BA}^x(r)$  follow  $g_{BA}^x(r) = 2 - g_{AA}^x(r)$  because  $\bar{\rho}_A = \bar{\rho}_B$  so that  $g_{AA}^x + g_{BA}^x = 2$ . If reactants  $A$  and  $B$  distribute homogeneously, the values of  $g_{AA}$  and  $g_{BA}$  should be equal to 1. Thus the result  $g_{AA} > 1$  directly shows that correlations

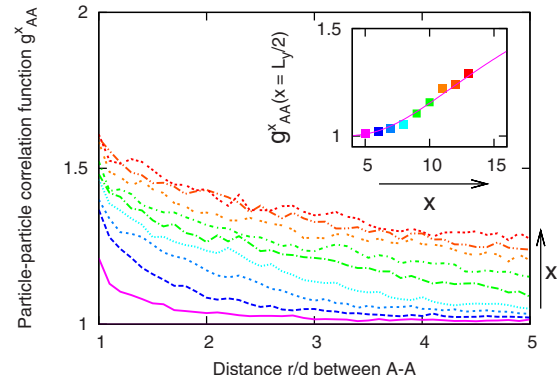


FIG. 3. (Color online) Particle-particle correlation functions  $g_{AA}^x(r)$ . In the direction of the arrow,  $g_{AA}^x$  for  $x=5, 6, \dots, 13$  are shown. The right end  $r=5$  is equal to  $L_y/2$ . In the inset, we show the values at  $r=L_y/2$  as a function of  $x$ . They are fitted by  $f(x) = 1 + \frac{C_1}{x} \exp(-C_2/x)$  with  $C_1=11.4$  and  $C_2=31.6$ .

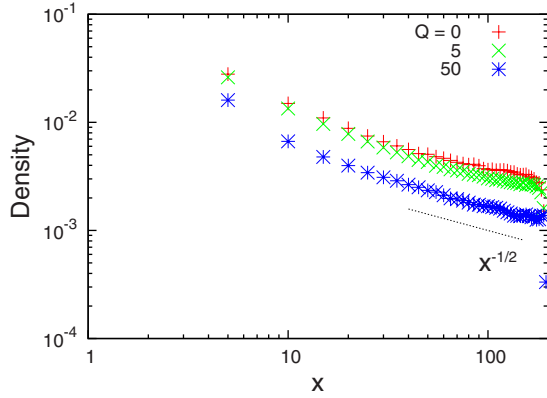


FIG. 4. (Color online) Distribution of reactant  $A$  in the reaction  $A+B=C+D+Q$  with energy release  $Q$  in two dimensions for different  $Q$ . The densities asymptotically approach  $x^{-1/2}$ .

between the same kind of reactants are stronger, i.e., a segregation. We can also see that the correlation length increases as  $x$  increases. The right end  $r=5$  is equal to  $L_y/2$  in the figure. In the inset, we show the values of  $g_{AA}^x$  at the end as a function of  $x$ . The plots can be fitted by a function  $f(x) = 1 + \frac{C_1}{\sqrt{x}} \exp(-C_2/x)$ , where  $C_1$  and  $C_2$  are parameters. This function describes one dimensional diffusion. Diffusion in one dimensional systems is given by  $g(y, t) = \frac{1}{\sqrt{t}} \exp(-y^2/t)$  so that at a fixed point  $y = \text{const}$  and  $x \sim t$ , it depends on  $x$  as  $g(x) = \frac{1}{\sqrt{x}} \exp(-1/x)$ . Therefore the correlation length grows by diffusion.

The power-law decays of  $-1/2$  and  $-3/4$  are explained as follows. As particles flow in the  $x$  direction with a constant average velocity  $v$ , particles diffuse as in the isotropic case if we observe the system from a reference frame which moves in the  $x$  direction. In  $d$ -dimensional isotropic systems, particles  $A$  and  $B$  will diffuse in volume  $V \sim t^{d/2}$  during time  $t$ . After time  $t$ , the number of remaining particles  $A$  or  $B$  is of the order  $\sqrt{V} \sim t^{d/4}$ . Therefore, the density decays as  $\sqrt{V}/V \sim t^{-d/4}$ . In our system, particles move in the  $x$  direction by  $x \sim vt$ . Therefore, the densities decay as  $\rho_A = \rho_B = x^{-d/4}$ .

So far, we considered irreversible reactions, however, in general a reaction will proceed in both directions. The reaction is approximately one directional as  $A+B \rightarrow C+D$  if the energy barrier from  $C+D$  to  $A+B$  is sufficiently high compared to the opposite direction. In reality, such a condition is realized when the internal energy state of reactants  $A$  and  $B$  is high and the reactions are exothermic. Our model does not include internal information of particles; however, we can include the energy release as follows. In our reaction processes, we release energy  $Q$  as  $K_A + K_B + Q = K_C + K_D$ , where  $K_i$  denotes a kinetic energy of species  $i$  in the center of mass reference frame. In Fig. 4, we show the distributions of reactants when the reaction is exothermic in two dimensions. As we can see, the densities asymptotically decay as  $x^{-1/2}$ .

We also confirm that the segregation changes the average distribution of reactants by simulating a system of reaction  $2A \rightarrow 2C$  in two dimensions. In the same manner as in the  $A+B$  case, particles of reactants  $A$  and products  $C$  are controlled in the left and right slices, respectively. In Fig. 5, we show distributions of reactants  $A$  in the steady state. As we

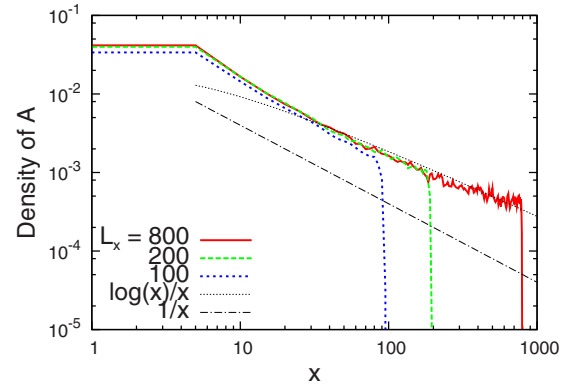


FIG. 5. (Color online) Distribution of particles in  $2A \rightarrow 2C$ . The line  $x^{-1}$  is shown as the mean-field solution. Reactant  $A$  of reactions  $2A$  appears to decay slightly slower and approach  $\log(x)/x$ .

can see, the distribution approaches  $\log(x)/x$ . The reactant of the  $2A$  reaction decays faster than that of  $A+B$  and it appears to decay slightly slower than the mean-field solution  $x^{-1}$ . This logarithmic correction is observed in isolated systems using hard spheres [9] as  $\log(t)/t$  and it is due to the marginal behavior of two dimensional diffusion in which depletion of reactants occur. In our geometry, we confirm that the correction is observed in the flow.

By using our geometry, we also directly observe anomalous behavior of the diffusion constant in the two dimensional system. We fix  $\bar{\rho}_L = \bar{\rho}_R = \bar{\rho}$  in the particle reservoirs and switch off the reaction processes. Let us consider a case in which  $A$  and  $C$  particles are added at the left and right slices, respectively. Here, we do not consider reactions so that collisions of  $A$  particles do not change them into  $C$  particles. Further, the densities for left and right slices are identical so that no macroscopic flow appears in this case; particles just diffuse by collisions with other particles. In Fig. 6, we show the results. As seen in the inset, we confirm that the average density of  $A$  particles,  $\rho_A(x)$  decreases linearly from  $x=0$  while that of  $C$  particles,  $\rho_C(x)$  increases keeping  $\rho_A(x) + \rho_C(x) = \bar{\rho}$ . The diffusion flux  $J_A = \rho_A(x)v_x$  for  $A$  particles has a constant positive value in the  $x$  direction while that of  $C$  has a negative one fulfilling  $J_A + J_C = 0$ . We confirm that the diffusion constant  $D_x = -J_A / \nabla \rho_A$  shows logarithmic dependence on the system size  $L_x$  in two dimensions. This behav-

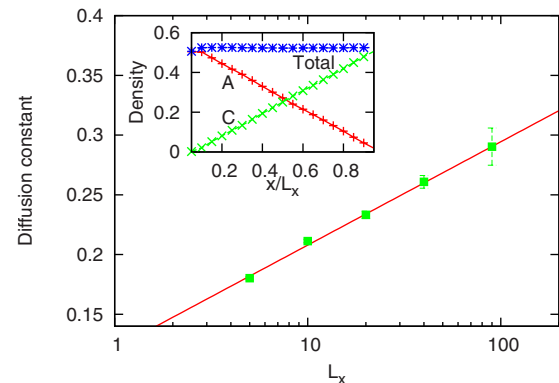


FIG. 6. (Color online) Dependence of the diffusion constant on system size.

ior is explained using the Green-Kubo formula [14] and long-time tail behavior  $t^{-d/2}$  of the autocorrelation function of velocities [15]. The density of  $A$  particles in our system shows linear profiles so that the macroscopic transport coefficient is written as an integral of velocity autocorrelation functions over time  $t$ , which is commonly known as the Green-Kubo formula. In a finite system, the upper limit of the integral is proportional to the system size  $L_x$ . Consequently, the integral of the autocorrelation function,  $t^{-d/2}$  depends on  $L_x$  as  $\log(L_x)$  in two dimensions. In three dimensions, the diffusion constant converges to a constant as confirmed in our simulations.

#### IV. SUMMARY

In this paper, we have shown that fluctuations are relevant to chemical reactions in flows producing anomalous spatial distributions. By attaching particle reservoirs, we simulate open systems with inflow and outflow of particles in two and three dimensions. In the case of  $A+B$ , segregations of reactants are observed and spatial distributions of reactants show power-law decay. In the case of  $2A$ , a logarithmic correction to the distribution is found. The logarithmic divergence of the diffusion constant is also confirmed.

In flowing stream, a power-law spatial distribution is observed and the power sensitively depends on the spatial dimension and the type of the reactions. In practical applications, the distribution is relevant to the efficiency of collecting products and the design of reactors, especially in the reaction miniaturizations to smaller scales. Our study presents essential behavior of flowing reaction-diffusion systems especially at nanoscale and microscale and gives fundamental guidelines for accurate measurement and control of such systems.

We remark that for the system studied in this paper periodic boundary conditions are imposed in the perpendicular directions to the stream. In chemical channels, walls in the short directions ( $y, z$ ) produce more restricted situations, i.e., quasi-one-dimensional geometry. In fact, studies on lattice-based models show crossover behavior in the scaling [5], and it will be the next step to examine these effects.

#### ACKNOWLEDGMENTS

A.K. acknowledges support from International Academic Exchange Grant Program of the University of Tokyo and the Japan Society for the Promotion of Science. N.I. is supported by the Japan Society for the Promotion of Science (Grant No. 19340110) and KAUST, GRP (Grant No. KUK-I1-005-04).

- 
- [1] For review, see P. Watts and C. Wiles, *Chem. Commun. (Cambridge)* **2007**, 443.
- [2] A. A. Ovchinnikov and Ya. B. Zeldovich, *Chem. Phys.* **28**, 215 (1978).
- [3] D. Toussaint and F. Wilczek, *J. Chem. Phys.* **78**, 2642 (1983).
- [4] R. Kopelman, *Science* **241**, 1620 (1988).
- [5] A. L. Lin, R. Kopelman, and P. Argyrakis, *J. Phys. Chem. A* **101**, 802 (1997).
- [6] L. K. Gallos and P. Argyrakis, *Phys. Rev. Lett.* **92**, 138301 (2004).
- [7] A. Kamimura, S. Yukawa, and N. Ito, *J. Phys. Soc. Jpn.* **74**, 1071 (2005).
- [8] A. Kamimura, S. Yukawa, and N. Ito, *J. Phys. Soc. Jpn.* **75**, 024005 (2006).
- [9] F. Baras, M. Salazar, E. Kestemont, and M. Malek Mansour, *Europhys. Lett.* **67**, 900 (2004).
- [10] H. van Beijeren, R. Kutner, and H. Spohn, *Phys. Rev. Lett.* **54**, 2026 (1985).
- [11] S. A. Janowsky, *Phys. Rev. E* **51**, 1858 (1995).
- [12] I. Ispolatov, P. L. Krapivsky, and S. Redner, *Phys. Rev. E* **52**, 2540 (1995).
- [13] T. Shimada, T. Murakami, S. Yukawa, K. Saito, and N. Ito, *J. Phys. Soc. Jpn.* **69**, 3150 (2000).
- [14] R. Kubo, *J. Phys. Soc. Jpn.* **12**, 570 (1957).
- [15] B. J. Alder and T. E. Wainwright, *Phys. Rev. A* **1**, 18 (1970).